Indian Journal of Experimental Biology
Vol. 61, October 2023, pp. 753-760
DOI: 10.56042/ijeb.v61i10.1653

Synthesis of silver nanoparticles using *Quillaja saponaria* Molina bark extract and its antivenom activities

Poulami Parua[1], Kanchan Saha[2], Sumana Sarkhel[2*], Upasana Chatterjee[3], Nuzhat Ara Jamal[1] & Simi Manna Pradhan[4]

[1]Centre for Life Science, Vidyasagar University, Paschim Medinipur-721 102, West Bengal, India
[2]Department of Human Physiology with Community Health; [3]Department of Microbiology; [4]Department of Biomedical Laboratory Science & Management, Vidyasagar University, Paschim Medinipur-721 102, West Bengal, India

Received 31 January 2023; *revised 29 April 2023*

Snakebite is an issue of concern, especially in India which accounts for half of the global deaths due to venomous snakebites every year. Saponins are glycosides of triterpenes and steroids known for their antivenom properties. The soap bark tree or Quillaya, *Quillaja saponaria* Molina represents the major resource of saponins for commercial applications. Here, we investigated the antivenom property of silver nanoparticle mediated saponins (AgNP-SP) from the *Q. saponaria* bark extract. AgNP-SP was prepared conducive to optimal temperature, pH of extract and concentration of $AgNO_3$. UV-VIS, FT-IR, XRD, TEM and SEM interpretations were devised to characterize AgNP-SP. AgNP-SP was tested for its efficacy to neutralize venom lethality and increase in myotoxicity biomarkers (LDH) in animal models. AgNP-SP was synthesized optimally at a concentration of 50 mg/mL, extract (pH 6.8) and temperature (80°C) with $AgNO_3$ (1 mM). The colour change and synthesis of AgNP-SP was examined by UV–Vis analysis at 430 nm. TEM studies showed the size for AgNP-SP to be 74.4 nm. FT-IR analysis showed peaks of AgNP-SP at 3422 cm^{-1} and 2926 (O–H stretching), 2358 cm^{-1} (O=C=O stretching), 1616 cm^{-1} (C=C stretching), 1097 cm^{-1} (C–F stretching), 813 cm^{-1} (C–CL stretching) and 651 cm^{-1} (C–Br stretching). The EDAX established the purity of the AgNP-SP. The biosynthesized AgNP-SP could significantly neutralize *Vipera russelli* venom (VRV) mediated elevation of biomarkers lactate dehydrogenase (LDH), serum glutamate pyruvate transaminase (SGPT) serum glutamic-oxaloacetic transaminase (SGOT), serum creatinine and serum uric acid. The present study, thus promulgates the therapeutic potential of silver nanoparticle mediated saponins (AgNP-SP) in ameliorating the biochemical and pharmacological effect of haemotoxic snake venom in animal models.

Keywords: Haemotoxic venom, Myotoxicity, Quillaya, Russell's viper, Saponins, Silver nanoparticles, Snake envenomation, Snakebite, Soap bark tree, *Vipera russelli* venom

Snakebites are accountable for a significant degree of disability and death worldwide, particularly in low resource countries. Half of the global deaths due to venomous snakebites, estimated at 100,000 per year, occur in India[1].

Snakebite envenoming is potentially life threatening. Inadequate past efforts to control snakebite envenoming has produced fragmented, inaccurate epidemiological data. Many victims do not attend health centres or hospitals and instead rely on traditional treatments. An ongoing crisis restricting access to antivenom treatment in many regions contributes to the predisposition of seeking help from traditional medicine.

Quillaja saponaria Molina represent the major resource of saponins for commercial applications. *Q. saponaria* triterpenoids are well-known for their significance due to their biological activities. Saponins are glycosides of triterpenes and steroids[2]. The amphiphilic structure of saponins could be attributed to their lipophilic aglycones and hydrophilic saccharide side chains[3,4].

The antivenom potential of saponins has not been studied much in detail. Therefore, in the present study, we investigated the therapeutic potential of silver nanoparticle based saponins (AgNP-SP) in ameliorating the pathophysiological changes induced by viper venom in both *in vitro* and *in vivo* models.

Materials & Methods

Venom Antiserum and Plant material

Viper russelli venom was procured from Calcutta Snake Park, Barasat, Kolkata and concentration was

*Correspondence:
Phone: +91 9836005398 (SS); +91 7003728402 (PP)
E-Mail: sumana.sarkhel@yahoo.in (SS);
poulamiparua1993@gmail.com (PP)

expressed in dry weight (mg/mL). The venom was kept at 8°C for 12 h. The antiserum was commercially purchased from VINS Bioproduct Ltd, Hyderabad, and the saponins derived from the bark of soap bark tree *Quillaja saponaria* Molina was purchased commercially from Sigma, Aldrich, India.

Chemicals

$AgNO_3$(Sigma), R D kits from Coral, India, NaCl (Sigma, India), ELISA kit (R& D; Thermofisher Scientific; India).

Silver nanoparticle synthesis with *Quillaja saponaria* bark extract

The dried methanolic plant material was treated with distilled water and expressed at concentration of 50 mg/mL. The plant material to metal ion were varied at concentrations (10:1, 40:1, 50:1 & 60:1). Precisely, 1 mM $AgNO_3$ was optimal for the preparation. $AgNO_3$ at a concentration of 1 mM was prepared[5]. AgNP-SP was prepared by mixing plant extract (4 mL) with 0.4 mL of 1 mM $AgNO_3$ and 15.6 mL distilled water in the volume of 20 mL and heated at 80°C and stirred at 550 rpm (Tarson: Digital Spinot) until the solution changed from yellowish to dark brown. The cooled solution was separated at 5000 rpm for 10 min. The collected pellets were used in this study[6]. The AgNP-SP could be used for three months.

Animals

Male Swiss albino mice (18±2) g were purchased from neighbouring dealer. Animal experiments were authenticated by the Vidyasagar University Animal Ethical Clearance Committee (IAEC) and in accordance with the Committee for the Purpose of Control and Supervision of Experiments (CPCSEA), Government of India (clearance no. VU/IAEC/CPCSEA/ 07/06/2022). Animals were maintained in standard cages with food pellets. Animal allocation for each group was done as per Table 1.

Optimization of parameters for synthesis of AgNP-SP

Optimization of extrinsic variables is critical for reaction parameters. UV–Vis study was performed to obtain optimum wavelength for AgNP-SP.

pH for formation of AgNP-SP

pH was varied from 5 to 9 with a difference of 1 to estimate the optimal pH of AgNP-SP.

$AgNO_3$ concentration

The concentration of AgNO3 was varied from 0.5-3.0 mM to optimize the synthesis of AgNP-SP. Zhang *et al*.[7] earlier reported optimum biosynthesis of AgNP could be achieved at a concentration of AgNO3 (1 mM). Concentration of $AgNO_3$ for production of AgNP-SP was selected by UV–Vis absorption spectroscopy.

Table 1 — Group wise animal allocation

Groups (n=6)	Treatment with doses (*i.v.*)
I	Saline control (0.9%) (*w/v*)
II	Venom control *(*VRV)(1 µg)
III	Venom (1 µg) + SP extract (4 mg/kg body wt.)
IV	Venom (1 µg) + AgNP-SP (1.5mg/kg; body wt.)
V	Venom (1 µg) + AVS (2 mg/mL) (50 µL)

Optimum temperature for AgNP-SP formation

The temperature was varied from 20 to 80°C with a difference of 10°C to see the effect on the formation of AgNP-SP.

Characterization of AgNP-SP

UV–Vis analysis

The colour change of AgNP-SP derived from *Quillaja saponaria* was studied by Shimadzu 1800 (Shimadzu Corporation, Kyoto, Japan) and the spectra was taken after 24 h after adding $AgNO_3$ (430 nm)[8].

FT-IR analysis

FT-IR studies of AgNP-SP was done with FT-IR spectrometer (Perkin-Elmer Spectrum Two).

Transmission electron microscopy (*TEM*)

TEM studies were performed with the sample using (JEM 2100 JEOL JAPAN instrument) at Central Instrumentation Facility; IIT Kharagpur.

X-ray diffraction study (*XRD*)

AgNP-SP was characterized by XRD ("X" Pert PRO PAN alytical, Netherlands). DLS and zeta potential activity AgNP-SP was dispersed in deionised water. It was centrifuged for 15 min at 25°C with 5000 rpm and the supernatant was collected. The particle distribution was examined in ZETA sizer Nanoseries, Malvern instrument Nano Zs 90.

Scanning electron microscopy and EDAX

AgNP-SP was characterized by SEM analysis performed by ZEISS EVO 60; ESEM, Model 8113 (Made in England). EDAX analysis was performed using EDX in SEM (Oxford INCA Penta FETX3)[9].

***In vivo* and *in vitro* venom neutralization assay**

Lethal and haemorrhagic action of VRV

The lethal MLD (Minimum lethal dose), MHD (haemorrhagic action), defibrinogenating action and MED (edema action) of VRV was investigated following method of Theakston & Reid[10].

Phospholipase A2 activity (*in vitro*)

Phospholipase A2 activity of *Vipera russelli* venom (VRV) was estimated following method of Habermann & Neumann[11].

Biochemical analysis of biomarkers

For biochemical analysis, Swiss albino mice (18±2 g) were categorized into 6 groups (6 animals each). Group I (0.9% *w/v* saline control) and Groups II, III, IV and V were treated with 1 µg VRV (i.v.). Group V received incubate of Viper venom VRV (1 µg) and antiserum (2 mg/mL). Groups III and IV received venom (1 µg) and *Quillaja saponaria* bark aqueous (4 mg/kg body wt.) and AgNP-SP (1.5 mg/kg body wt.) incubate respectively. 4 h after blood collection from animals (from retro-orbital plexus), blood was allowed to clot for 30 min at 37°C. Colorimetric estimation of serum glutamate pyruvate transaminase (SGPT) and serum glutamic-oxaloacetic transaminase (SGOT) were performed by the method of Reitman & Frankel[12].

Serum creatinine was estimated by method of Toro *et al.*[13] where the intensity of orange coloured complex formed by reacting alkaline picrate with creatinine was colorimetrically estimated.

Statistical analysis

Results are shown as Mean ± SD. Results were analyzed using one way ANOVA. The difference was given as statistically significant at P <0.05 are compared to venom control.

Results and Discussion

The overall yield of the plant extract was only a meagre 2%. The synthesized AgNP-SP was dark brown in colour and stable for 90 days at 8±2°C (Fig. 1). The optimum concentration of *Quillaja saponaria* Mol bark for nanoparticle synthesis was 50 mg/mL. The pH of the solution medium is an important parameter that influences the rate, shape and size of the biosynthesized AgNP. In the present study, we have observed that AgNP-SP was optimally synthesized at a pH 8. An earlier report has shown that alkaline pH is ideal of AgNP synthesis which corroborates our present findings[14]. This is attributed to the presence of larger number of functional groups at higher pH leading to nucleation. Nucleation increases with increase in solution pH indicating the formation of Ag^{o} from Ag+ due to bio-reduction .

UV–VIS analysis

UV–Vis spectra of AgNP-SP showed localized Plasmon resonance of AgNP (Fig. 1). AgNP-AS turned dark brown on addition of $AgNO_3$. UV- Vis spectrophotometric analysis is carried out for the primary investigation of silver nanoparticle synthesis. Earlier studies recorded illustrated surface plasmon resonance of silver nanoparticles ranging from 422-430 nm[15]. In this study, after mixing extract with silver nitrate solution a colour change was observed over the progression of time due to the reduction of silver ions. UV-Vis studies were carried out and a peak was observed at 430 nm which showed a stable range for nanoparticle formation. The absorption of AgNPs depends on the particle size, dielectric medium and chemical surroundings. In AgNPs, the conduction band and valence band lie very close to each other in which electrons move freely. These free electrons give rise to surface plasmon resonance absorption band occurring due to collective oscillations of electrons of silver nanoparticles in resonance with light wave.

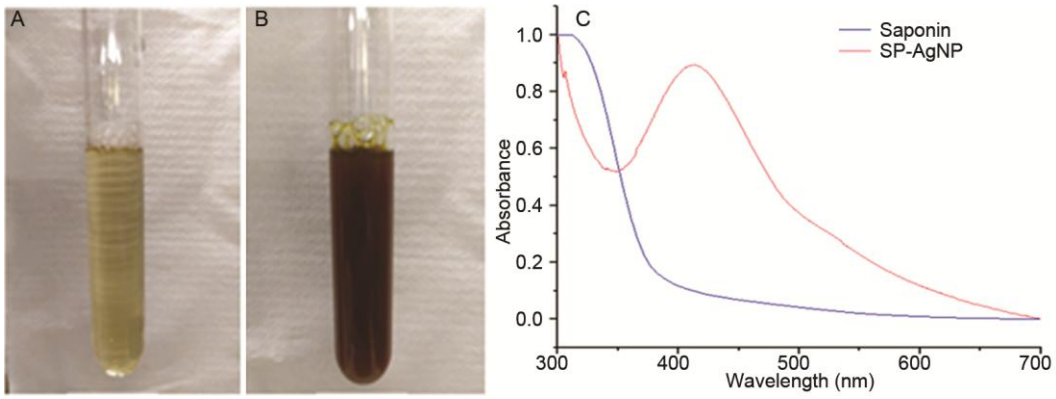

Fig. 1 — The UV-Vis absorption spectra of saponin extract (SP) and silver nanoparticles of saponins (AgNP-SP) indicating colour change. (A) Saponin extract (SP); (B) Silver nanoparticles of saponins (AgNP-SP); and (C) UV–Vis spectra of silver nanoparticle based *Quillaja saponaria* bark extract (AgNP-SP).

FT-IR analysis

FT-IR spectra of saponin shows peaks varying at 3425 cm^{-1} (O–H stretching), 2943 cm^{-1} (N–H stretching), 1733 cm^{-1} (C=O stretching), 1639 cm^{-1} (C=C stretching), 1073 cm^{-1} (S=O, 646 cm^{-1} (=C–Br bending) and FT-IR analyzed peaks of AgNP-SP at 3422 cm^{-1} and 2926 (O–H stretching), 2358 cm^{-1} (O=C=O stretching), 1616 cm^{-1} (C=C stretching), 1097 cm^{-1} (C–F stretching), 813 cm^{-1} (C–CL stretching), 651 cm^{-1}(C–Br stretching) (Fig. 2). FT-IR is carried out to identify the presence of various functional groups in biomolecules responsible for bioreduction of silver and capping and stabilizing of silver nanoparticles[16]. FT-IR has been extended to study the nano-scaled materials such as the confirmation of functional groups covalently grafted onto silver.

Transmission electron microscopic studies and EDAX analysis

Transmission electron microscopy shows measured average particle size for AgNP-SP of 74.4 nm (Fig. 3). Different capping agents in the extracts has been reported earlier. The EDAX indicated a peak for silver. EDX spectrum reveals strong signal in the silver region and confirms of the formation of AgNP. Metallic silver nanocrystals generally show typical optical absorption peak at 3KeV due to surface plasmon resonance[17].

X-ray diffraction studies

X-ray diffraction pattern of AgNP-SP had Bragg's reflections of planes, which confirms the face-centered cubic (FCC) crystalline structure of silver (Fig. 4). Four Bragg's reflections confirming to (111), (200), (220), (311) planes of metallic silver with FCC crystal structure could be understood clearly from the XRD plot. In the present study, the crystalline nature of nanoparticles has been confirmed by X-ray crystallography. The results ascribed from XRD pattern are in good agreement for the face centred cubic (FCC) structure of AgNP as described in earlier studies[18]. The diffracted pattern also confirms whether the sample material is pure.

Dynamic light scattering

The hydrodynamic diameter of AgNP-SP was 74.4 nm (Fig. 5 A & B). The zeta potential of AgNP-SP (−8.55 mV). The size distribution and zeta potential of AgNP-SP has been determined by DLS. A negative potential value supports long term stability, good colloidal nature and high dispersity of

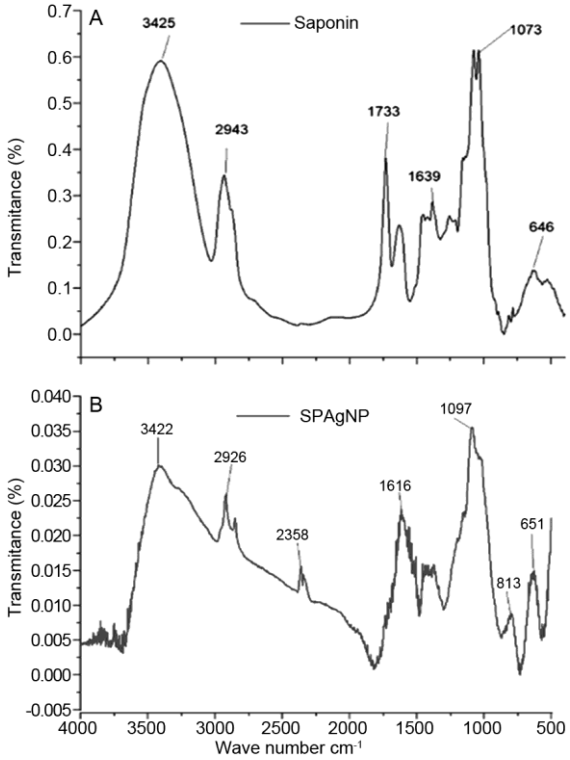

Fig. 2 — FT-IR analysis of silver nanoparticle based *Quillaja saponaria* bark extract (AgNP-SP). (FT-IR of (A) crude extract (SP); and (B) AgNP-SP.

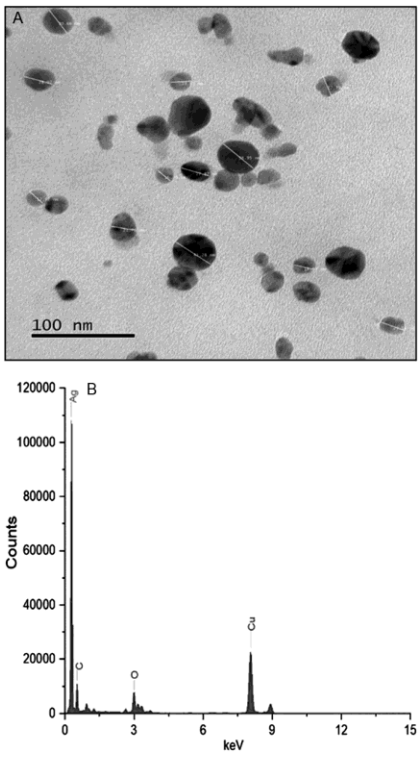

Fig. 3 — (A) Transmission Electron microscopic image; and (B) EDAX analysis of AgNP-SP

AgNPs due to negative-negative repulsion[19]. DLS measures the light scattered from a laser that passes through the colloid, and mostly relies on Rayleigh scattering from suspended nanoparticles. The modulation of scattered light intensity as a function of time is analyzed and the hydrodynamic diameter is determined. The size obtained from DLS is usually larger than transmission electron microscope which may be due to the influence of Brownian motion.

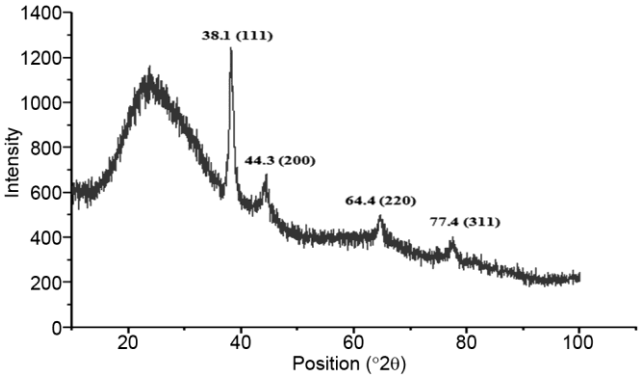

Fig. 4 — X-ray diffraction of silver nanoparticle based *Quillaja saponaria* bark extract (AgNP-SP)

Scanning electron microscopy

Figure 6 illustrates the SEM studies of AgNP-SP. SEM studies provided further insight into the morphology and size of the AgNPs[20]. SEM is a surface imaging method fully capable of resolving different particle sizes, size distributions and surface morphology of synthesized nanoparticles.

***In vivo* and *in vitro* venom neutralization assay of *Quillaja saponaria* bark extract and AgNP-SP**

The LD_{50} of VRV was found to be 1.75 µg. AgNP-SP gave up to 2 fold protection against VRV induced lethality (MLD), 3 fold against edema (MED), 1.7 fold against defibrinogenation (MDD), 1.5 fold against haemorrhage (MHD) and 2 fold against PLA_2 activity (Table 2).

Neutralization of venom induced changes in serum biomarkers

AgNP-SP conjugated with VRV gave 65 and 63% protection against venom induced rise in SGOT and SGPT.

In similar studies, saponin extract conjugated with venom gave 42 and 58% inhibition of venom induced rise in SGOT and SGPT. AgNP-SP conjugated with VRV provided 48, 73 and 64% inhibition of viper

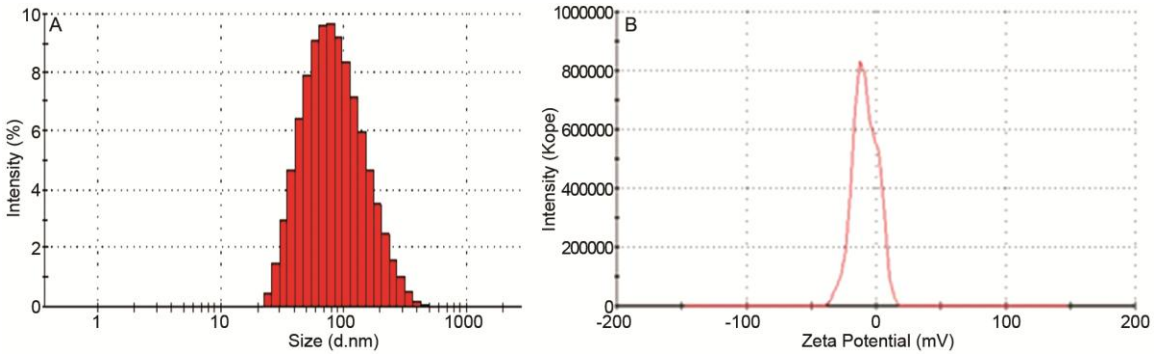

Fig. 5 — (A) Dynamic light scattering of hydrodynamic diameter (74.4 nm); and (B) zeta potential (−8.55 mV) of AgNP-SP.

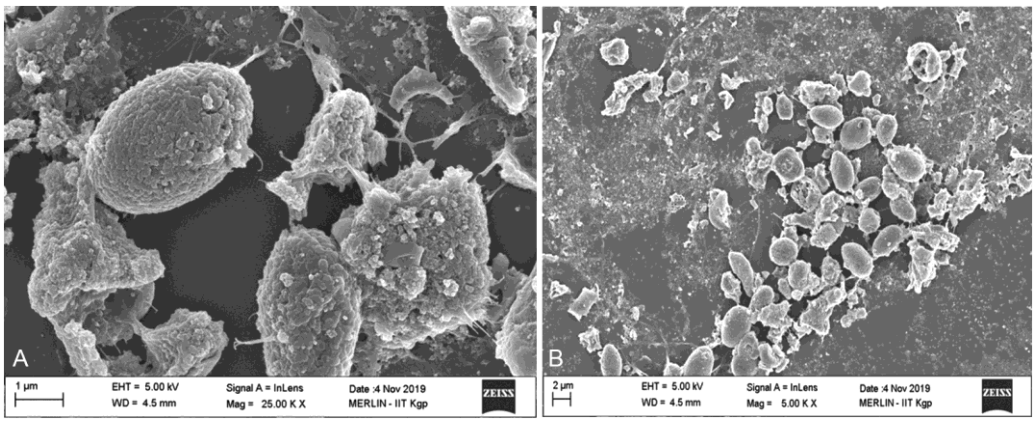

Fig. 6 — (A) SEM pictures of silver powder granulates deposited on carbon strip and (B)SEM image of AgNP-SP

Table 2 — *In vivo* and *in vitro* venom neutralization studies of *Quillaja saponaria* bark extract and AgNP-SP

N=6	Group II VRV (µg)	Group III VRV (µg) + SP (mg/kg body wt.) (fold of protection, P/NP)	Group IV VRV (µg) + AgNP-SP (1.5 mg/kg body wt.) (fold of protection)
Minimum lethal dose (MLD) (i.v.)	VRV (2 µg) [1 MLD]	VRV (2 µg) + SP (4 mg/kg body wt.) (1 fold, P) VRV (4 µg) + SP (4 mg/kg body wt.) (2 fold, NP)	VRV (2 µg) + SP (1.5 mg/kg body wt. (1 fold, P) VRV (4 µg) + SP (1.5 mg/kg body wt.) (2 fold, NP) VRV (6 µg) + SP (1.5 mg/kg body wt.) (3 fold, NP)
Minimum lethal dose (MLD) (s.c)	VRV (15 µg) [1 MLD]	VRV (15 µg) + SP (4 mg/kg body wt.) (1 fold, P) VRV (25 µg) + SP (4 mg/kg body wt.) (1.67 fold, P) VRV (30 µg) + SP (4 mg/kg body wt.) (2 fold, NP)	VRV (15 µg) + SP (1.5 mg/kg body wt.) (1 fold, P) VRV (25 µg) + SP (1.5 mg/kg body wt.) (1.67 fold, P) VRV (30 µg) + SP (1.5 mg/kg body wt.) (2 fold, P) VRV (35 µg) + SP (1.5 mg/kg body wt.) (2.33 fold, NP)
Minimum edema dose (MED)	VRV (1 µg) (1 MED)	VRV (1 µg) + SP (4 mg/kg body wt.) (1 fold, P) VRV (2 µg) + SP (4 mg/kg body wt.) (2 fold, P) VRV (3 µg) + SP (4 mg/kg body wt.) (3 fold, NP)	VRV (1 µg) + SP (1.5 mg/kg body wt.) (1 fold, P) VRV (2 µg) + SP (1.5 mg/kg body wt.) (2 fold, P) VRV (3 µg) + SP (1.5 mg/kg body wt.) (3 fold, P) VRV (4 µg) + SP (1.5 mg/kg body wt.) (4 fold, NP)
Minimum defibrination dose (MDD)	VRV (1.75 µg) [1 MDD]	VRV (1.75 µg) + SP (4 mg/kg body wt.) (1 fold, P) VRV (2.5 µg) + SP (4 mg/kg body wt.) (1.4 fold, P) VRV (3 µg) + SP (4 mg/kg body wt.) (1.71 fold, NP)	VRV (1.75 µg) + SP (1.5 mg/kg body wt.) (1 fold, P) VRV (2.5 µg) + SP (1.5 mg/kg body wt.) (1.4 fold, P) VRV (3 µg) + SP (1.5 mg/kg body wt.) (1.71 fold, P) VRV (3.5 µg) + SP (1.5 mg/kg body wt.) (2 fold, NP)
Minimum hemorrhagic dose (MHD)	VRV (10 µg) [1 MHD]	VRV (10 µg) + SP (4 mg/kg body wt.) (1 fold, P) VRV (15 µg) + SP (4 mg/kg body wt.) (1.5 fold, NP)	VRV (10 µg) + SP (1.5 mg/kg body wt.) (1 fold, P) VRV (15 µg) + SP (1.5 mg/kg body wt.) (1.5 fold, P) VRV (20 µg) + SP (1.5 mg/kg body wt.) (2 fold, NP)
PLA_2	VRV (0.1 µg) [1 unit]	VRV (0.1 µg) + SP (4 mg/kg body wt.) (1 fold, P) VRV (0.2 µg) + SP (4mg/kg body wt.) (2 fold, NP)	VRV (0.1 µg) + SP (1.5 mg/kg body wt.) (1 fold, P) VRV (0.2 µg) + SP (1.5 mg/kg body wt.) (2 fold, P) VRV (0.3 µg) + SP (1.5 mg/kg body wt.) (3 fold, NP)

[P: Protection; NP: No Protection; VRV: *Vipera russelli* venom; SP: ;Saponin extract.

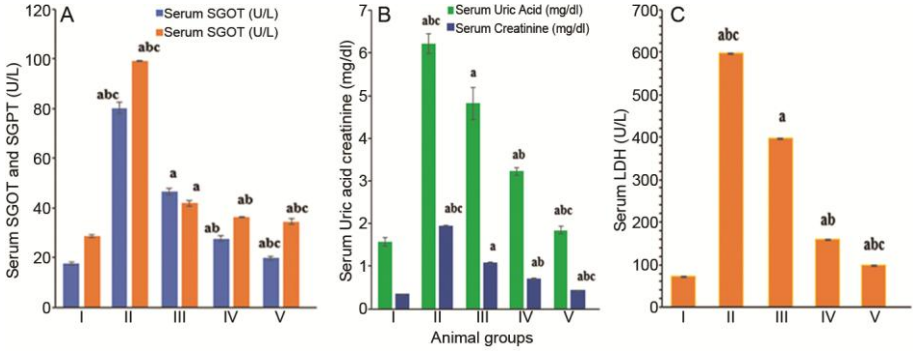

Fig. 7 — VRV induced rise in (A) serum uric acid (mg/dL) and creatinine (mg/dL); (B) serum LDH (U/L); and (C) serum SGOT (U/L) and SGPT (U/L). [Neutralization by saponin (SP), Silver nanoparticles of saponins (AgNP-SP) and antivenom (AVS). ^{a}P <0.05 when compared Gr. II with Gr. III, ^{ab}P <0.05 when compared Gr. II with Gr. IV, and ^{abc}P <0.05 when compared Gr. II with Gr. V]

venom induced rise in uric acid, LDH and creatinine. Whereas in Group III saponin extract conjugated with venom gave upto 22, 33.28 and 45% safety against venom induced rise in uric acid, LDH and creatinine (Fig. 7).

The present work attempts to investigate silver nanoparticle mediated saponin nanoparticles (AgNP-SP) were synthesized and characterized. The colour of AgNP-SP was changed into dark yellowish-brown colour solution[21,22]. Transmission electron microscopy (TEM) showed measured typical particle size for AgNP-SP of 74.4 nm[23]. The Bragg's reflections for AgNP-SP were (111), (200), (220) and (311) planes which confirms the face-centered cubic (FCC) crystalline structure of silver. FT-IR revealed peaks in the array of 3425 cm^{-1} (O–H stretching), 2943 cm^{-1} (N–H stretching), 1733 cm^{-1} (C=O stretching), 1639 cm^{-1} (C=C stretching), 1073 cm^{-1} (S=O, 646 cm^{-1} (=C–Br bending). In the FT-IR spectra of AgNP-SP, 3422 cm^{-1} and 2926 (O–H stretching), 2358 cm^{-1} (O=C=O stretching), 1616 cm^{-1} (C=C stretching), 1097 cm^{-1} (C–F stretching), 813 cm^{-1} (C–CL stretching), 651 cm^{-1} (C–Br stretching) were evident. From the dynamic light scattering studies, the hydrodynamic diameter (74.4 nm) and zeta potential (−8.55 mV) of AgNP-SP were estimated. The EDAX validated that AgNP-SP silver was pure. In an earlier study, a silver nanoparticle obtained by reducing salts with solid dispersion of curcumin was used to counteract against the toxic (edematogenic/myotoxic) and neurotoxic

effects of *Philodryas olfersii* venom[24]. In a report; Gomes et al. (2010) corroborated the venom inhibiting activity of Indian medicinal plants[25]. The whole seed extract of *Srychnos nux vomica* in low doses could effectively neutralize Daboia russelli venom mediated pathology[26]. In another study, *Canthium parviflorum*, a traditional plant used in treatment of snakebite could effectively ameliorate saw scaled viper venom induced edema and phospholipase A2 activity[27].

In the studies with serum biomarkers, AgNP-SP conjugated with VRV gave 65 and 63% protection from venom mediated elevation in SGOT and SGPT. AgNP-SP conjugated with VRV provided 48, 73 and 64% inhibition of viper venom mediated elevation in uric acid, LDH and creatinine.

This is the first report of antivenom potential of silver nanoparticle based saponin nanoconjugate (AgNP-SP). In Group V, antivenom provided significant inhibition of venom induced rise in uric acid (70%), creatinine (78%), LDH (83%), SGOT (75%) and SGPT (65%). In Group IV and V which are treated with AgNP-SP and antivenom respectively, AgNP-SP and antivenom provided comparable protection in venom-induced rise in uric acid, creatinine, LDH, SGOT and SGPT. Therefore, AgNP-SP can be a candidate molecule with promising antivenom potential. Further investigation may validate the findings and mode of action of AgNP-SP.

Snakebite envenomation is a debilitating condition that was lately re-included as a neglected tropical disease (NTD), affecting millions of people in tropical and subtropical areas globally. Improvement in the restorative approaches to envenomation is imperative to reduce the morbidity and mortality effects of this NTD. Antivenoms have been used to treat snake envenoming for more than a century. However, the effectiveness of antivenom therapy in preventing or reducing the local tissue damage in snake envenoming is not well-supported by current evidence[28].The present study is endeavoured to investigate the therapeutic potential of AgNP-SP in ameliorating venom induced pathophysiology.

Conclusion

In the present study, we synthesized silver nanoparticles AgNP-SP optimally using the soap bark tree or Quillaya, *Quillaja saponaria* and characterized it by UV–Vis, FT-IR, XRD, TE and SEM studies. We have further investigated the neutralization of *Vipera russelli* venom induced lethality, hepatoxicity, myotoxicity and nephrotoxicity through *in vitro* and *in vivo* models. The AgNP-SPs have shown significant protection comparable to antivenom against venom induced pathophysiology. Therefore, further work is warranted to develop this compound as a novel treatment therapy against snake envenomation.

Acknowledgement

The study was undertaken from the funds of Department of Science and Technology (Ref:607 (Sanc)/ST/P/S&T/5G-3/2016 dated 17/10/2016).

Conflict of Interest

Authors declare no competing interests.

References

1 Menon JC, Bharti OK, Dhaliwal RS, John D, Menon GR, Grover A & Chakma JK, ICMR task force project- survey of the incidence, mortality, morbidity and socio-economic burden of snakebite in India: A study protocol. *PLoS ONE*, 17 (2022) 270735.

2 Xu M, Wan Z & Yang X, Recent Advances and Applications of Plant-Based Bioactive Saponins in Colloidal Multiphase Food Systems. *Molecules*, 26 (2021) 6075.

3 Sharma P, Tyagi A, Bhansali P, Pareek S, Singh V, Ilyas A, Mishra R & Poddar NK, Saponins: Extraction, bio-medicinal properties and way forward to anti-viral representatives. *Food Chem Toxicol*, 15 (2021) 112075.

4 Augustin JM, Kuzina V, Andersen SB & Bak S, Molecular activities, biosynthesis and evolution of triterpenoid saponins. *Phytochemistry*, 72 (2011) 435.

5 Vanlalveni C, Lallianrawna S, Biswas A, Selvaraj M, Changmai B & Rokhum SL, Green synthesis of silver nanoparticles using plant extracts and their antimicrobial activities: a review of recent literature. *RSC Adv*, 11 (2021) 2804.

6 Salayova A, Bedlovicova Z, Daneu N, Balaz M, Lukacova Bujnakova Z, Balazova L &Tkacikova L, Green Synthesis of Silver Nanoparticles with Antibacterial Activity Using Various Medicinal Plant Extracts: Morphology and Antibacterial Efficacy. *Nanomaterials*, 11 (2021) 1005.

7 Zhang Y, Cheng X, Zhang Y, Xue X & Fu Y, Biosynthesis of silver nanoparticles at room temperature using aqueous aloe leaf extract and antibacterial properties. *Colloids Surf. A Physicochem Eng Asp*, 423 (2013) 63.

8 Hasan KF, Xiaoyi L, Shaoqin Z, Horvath PG, Bak M, Bejo L, Sipos G & Alpar T, Functional silver nanoparticles synthesis from sustainable point of view: 2000 to 2023–A review on game changing materials. *Heliyon*, 8 (2022) 12322.

9 Dada AO, Adekola FA, Dada FE, Adelani-Akande AT, Bello MO, Okonkwo CR, Inyinbor AA, Oluyori AP, Olayanju A, Ajanaku KO & Adetunji CO, Silver nanoparticle synthesis by *Acalypha wilkesiana* extract: phytochemical screening, characterization, influence of

operational parameters, and preliminary antibacterial testing. *Heliyon*, 5 (2019) 2517.
10 Theakston RD & Reid HA, Development of simple standard assay procedures for the characterization of snake venoms. *Bull World Health Organ*, 61 (1983) 949.
11 Habermann E & Neumann W, Egg yolk coagulation method. *Physiol Chem*, 297 (1954) 174.
12 Reitman S & Frankel S, A colorimetric method for the determination of serum glutamic oxalacetic and glutamic pyruvic transaminases. *Am J Clinic Pathol*, 28 (1957) 56.
13 Toro G & Ackermann PG, *Practical Clinical Chemistry*. (Little Brown and Co., Boston, USA), 1975, 354.
14 Huang H, Shan K, Liu J, Tao X, Periyasamy S, Durairaj S, Jiang Z & Jacob JA, Synthesis, optimization and characterization of silver nanoparticles using the catkin extract of Piper longum for bactericidal effect against food-borne pathogens via conventional and mathematical approaches. *Bioorg Chem*, 10 (2020) 104230.
15 Melkamu WW & Bitew LT, Green synthesis of silver nanoparticles using *Hagenia abyssinica (Bruce) J.F. Gmel* plant leaf extract and their antibacterial and anti-oxidant activities. *Heliyon*, 7 (2021) 2405.
16 Zhuang J, Li M, Pu Y, Ragauskas AJ & Yoo CG, Observation of Potential Contaminants in Processed Biomass Using Fourier Transform Infrared Spectroscopy. *Appl Sci*, 10 (2020) 4345.
17 Dilshad E, Bibi M, Sheikh NA, Tamrin KF, Mansoor Q, Maqbool Q & Nawaz M, Synthesis of Functional Silver Nanoparticles and Microparticles with Modifiers and Evaluation of Their Antimicrobial, Anticancer, and Antioxidant Activity. *J Funct Biomat*, 11 (2020) 76.
18 Ali MH, Azad MA, Khan KA, Rahman MO, Chakma U & Kumer A, Analysis of Crystallographic Structures and Properties of Silver Nanoparticles Synthesized Using PKL Extract and Nanoscale Characterization Techniques. *ACS omega*, 8 (2023) 28133.
19 Erdogan O, Abbak M, Demirbolat GM, Birtekocak F, Aksel M, Pasa S & Cevik O, Green synthesis of silver nanoparticles via *Cynara scolymus* leaf extracts: The characterization, anticancer potential with photodynamic therapy in MCF7 cells. *PloS ONE*, 14 (2019) 0216496.
20 Badar W, Ullah Khan MA, Analytical study of biosynthesised silver nanoparticles against multi-drug resistant biofilm forming pathogens. *IET Nanobiotechnology*, 14 (2020) 331.
21 Jalab J, Abdelwahed W, Kitaz A & Al-Kayali R, Green synthesis of silver nanoparticles using aqueous extract of *Acacia cyanophylla* and its antibacterial activity. *Heliyon*, 7 (2021) 2405.
22 Gong P, Li H, He X, Wang K, Hu J, Tan W, Zhang S & Yang X, Preparation and antibacterial activity of Fe_3O_4 Ag nanoparticles. *Nanotechnology*, 18 (2007) 285604.
23 John MS, Nagoth JA, Ramasamy KP, Mancini A, Giuli G, Natalello A, Ballarini P, Miceli C & Pucciarelli S, Synthesis of bioactive silver nanoparticles by a *Pseudomonas* strain associated with the antarctic psychrophilic protozoon *Euplotes focardii*. *Mar Drugs*, 18 (2020) 38.
24 Proença-Assuncao JD, Farias-de-França AP, Tribuiani N, Cogo JC, Collaco RD, Randazzo-Moura P, Consonni SR, Chaud MV, Santos CA & Oshima-Franco Y, The influence of silver nanoparticles against toxic effects of *Philodryas olfersii* venom. *Int J Nanomed*, 16 (2021) 3555.
25 Gomes A, Das R, Sarkhel S, Mishra R, Mukherjee S, Bhattacharya S & Gomes A, Herbs and herbal constituents active against snake bite. *Indian Journal of Experimental Biology*, 48(2010) 865.
26 Chatterjee I, Chakravarty AK & Gomes A, Antisnake venom activity of ethanolic seed extract of *Strychnos nux vomica* Linn. *Indian J Exp Biol*, 42 (2004) 468.
27 Vineetha MS, Janardhan B & More SS, Biochemical and pharmacological neutralization of Indian saw-scaled viper snake venom by Canthium parviflorum extracts. *Indian J Biochem Biophys*, 54 (2017) 173.
28 Madhushani U, Thakshila P, Hodgson WC, Isbister GK & Silva A, Effect of Indian polyvalent antivenom in the prevention and reversal of local myotoxicity induced by common cobra (*Naja naja*) venom from Sri Lanka *in vitro*. *Toxins*, 13 (2021) 308.